Molecular Biology of the Cell
Vol. 21, 4076–4088, December 1, 2010

Dysfunction of Heterotrimeric Kinesin-2 in Rod Photoreceptor Cells and the Role of Opsin Mislocalization in Rapid Cell Death

Vanda S. Lopes,*†‡ David Jimeno,†‡§ Kornnika Khanobdee,†‖ Xiaodan Song,† Bryan Chen,* Steven Nusinowitz,* and David S. Williams*†

*Departments of Ophthalmology and Neurobiology, UCLA School of Medicine, Los Angeles, CA 90095; and †Departments of Pharmacology and Neurosciences, UCSD School of Medicine, LA Jolla, CA 92130

Submitted August 23, 2010; Revised September 27, 2010; Accepted September 29, 2010
Monitoring Editor: Erika Holzbaur

Due to extensive elaboration of the photoreceptor cilium to form the outer segment, axonemal transport (IFT) in photoreceptors is extraordinarily busy, and retinal degeneration is a component of many ciliopathies. Functional loss of heterotrimeric kinesin-2, a major anterograde IFT motor, causes mislocalized opsin, followed by rapid cell death. Here, we have analyzed the nature of protein mislocalization and the requirements for the death of kinesin-2-mutant rod photoreceptors. Quantitative immuno EM showed that opsin accumulates initially within the inner segment, and then in the plasma membrane. The light-activated movement of arrestin to the outer segment is also impaired, but this defect likely results secondarily from binding to mislocalized opsin. Unlike some other retinal degenerations, neither opsin–arrestin complexes nor photoactivation were necessary for cell loss. In contrast, reduced rod opsin expression provided enhanced rod and cone photoreceptor survival and function, as measured by photoreceptor cell counts, apoptosis assays, and ERG analysis. The cell death incurred by loss of kinesin-2 function was almost completely negated by *Rho*$^{-/-}$. Our results indicate that mislocalization of opsin is a major cause of photoreceptor cell death from kinesin-2 dysfunction and demonstrate the importance of accumulating mislocalized protein per se, rather than specific signaling properties of opsin, stemming from photoactivation or arrestin binding.

INTRODUCTION

A variety of genes encode proteins that are critical for the formation and maintenance of cilia. These genes underlie ciliopathies, which are manifest in different organs, such as the retina, kidney, and the cerebellum. In the vertebrate retina, the phototransductive compartment of the photoreceptor cells, the outer segment, is formed by extensive amplification of the plasma membrane of a primary cilium. The resulting phototransductive disk membranes undergo continuous renewal (Young, 1967), requiring the delivery of large amounts of newly synthesized opsin-containing membrane along the ciliary axoneme. In addition to membrane proteins, some soluble signaling proteins, such as arrestin, transducin, and recoverin, relocate between the inner and outer segments in response to changes in light intensity (Strissel *et al*., 2006). Protein trafficking along the photoreceptor cilium is thus especially busy, and defects in ciliary trafficking appear to lead to rapid photoreceptor cell degeneration.

Anterograde transport in all primary cilia requires heterotrimeric kinesin-2 and associated intraflagellar transport (IFT) proteins (Rosenbaum and Witman, 2002; Scholey, 2008). Genetic studies have shown that mutations in *Kif3a* or *Kif3b*, the genes encoding motor subunits of heterotrimeric kinesin-2 (Marszalek *et al*., 2000; Lin-Jones *et al*., 2003; Jimeno *et al*., 2006; Avasthi *et al*., 2009), or mutant IFTs (Pazour *et al*., 2002; Krock and Perkins, 2008; Sukumaran and Perkins, 2009) cause an abnormal accumulation of opsin in the photoreceptor inner segment and nuclear layer, followed by photoreceptor cell death. Homodimeric kinesin-2, which consists of KIF17 subunits, is required for the formation of the disk membranes, and thus appears to function in a later stage of the delivery process (Insinna *et al*., 2008; Insinna *et al*., 2009). [In the remainder of this paper, kinesin-2 refers to heterotrimeric kinesin-2, which consists of the motor subunits, KIF3A and KIF3B or KIF3C, and a KAP3 subunit, according to standardized nomenclature (Lawrence *et al*., 2004.] In KIF3A-depleted photoreceptor cells, arrestin failed to localize in the outer segment in the light, suggesting that kinesin-2 might also transport soluble proteins to the outer segment (Marszalek *et al*., 2000).

The loss of photoreceptor cells due to disruption of IFT is particularly swift. The synchronous deletion of *Kif3a* from rod photoreceptor cells results in the death of nearly all cells within the ensuing 2 wk. The redistribution of opsin that

This article was published online ahead of print in *MBoC in Press* (http://www.molbiolcell.org/cgi/doi/10.1091/mbc.E10–08–0715) on October 6, 2010.

‡ V.S.L. and D.J. contributed equally to the study.

Present addresses: § Instituto de Neurociencias de Castilla y León, Salamanca, Spain; ‖ Institute of Science, Suranaree University of Technology, Muang, Nakhon Ratchasima, Thailand.

Address correspondence to: David S. Williams (dswilliams@ucla.edu).

precedes cell death has been suggested as a primary cause of the death (Marszalek *et al*., 2000). Supporting this notion, mutations in the rod opsin gene that affect its targeting also result in cell death (Sung *et al*., 1991; Sung *et al*., 1994; Li *et al*., 1996; Green *et al*., 2000; Chapple *et al*., 2001; Concepcion *et al*., 2002; Tam and Moritz, 2006). Moreover, some other mouse models of syndromic ciliopathies (e.g., *Rpgrip*, *Bbs2*, *Cep290*, *Ahi1* mutants) have now identified the mislocalization of opsin as a mutant phenotype preceding photoreceptor cell loss (Zhao *et al*., 2003; Nishimura *et al*., 2004; Chang *et al*., 2006; Louie *et al*., 2010). Nevertheless, an abnormal accumulation of opsin outside of the outer segment is not only associated with cell death in cases where the mistargeting of opsin is a primary lesion. It is a characteristic of photoreceptor cells before their death in a variety of retinal degeneration models, such as the *rd* and *rds* mice, and the *RCS* rat (Nir and Papermaster, 1986; Jansen *et al*., 1987; Nir *et al*., 1987; Usukura and Bok, 1987; Nir *et al*., 1989). These examples prompt the question of whether an abnormal accumulation of opsin is part of a requisite pathway leading to the cell death or is simply a secondary response in a dying photoreceptor cell.

In some cases, specific signaling from opsin has been suggested as necessary for cell death. A number of photoreceptor degenerations are light-dependent, suggesting the requirement of light activation of rhodopsin; although they may or may not require activation of the transducin-mediated phototransductive cascade (Hao *et al*., 2002). In cell culture studies with dissociated salamander retinas, light activation of mislocalized opsin appeared to elicit rod cell death through G protein stimulation of adenylate cyclase (Alfinito and Townes-Anderson, 2002), although in vivo studies with *Xenopus* showed that activation of mislocalized C-terminal truncated opsin was not required for cell death (Tam and Moritz, 2006). A proposed mechanism that does not require activation of the phototransductive cascade stems from genetics studies with Drosophila (Alloway *et al*., 2000; Kiselev *et al*., 2000). In these studies, the requirement of arrestin for degeneration was reported, suggesting signaling from phosphorhodopsin-arrestin complexes. More recently, the constitutively-active K296E opsin was found to bind arrestin and accumulate ectopically in transgenic mouse photoreceptors. The ensuing degeneration also appeared to result from transducin-independent signaling by opsin-arrestin complexes (Chen *et al*., 2006).

In the present study, we first dissected the time course of the mislocalization of opsin due to kinesin-2 dysfunction in a quantitative manner and thus describe a characteristic that is likely unique to a trafficking defect. Next, we addressed the possibility of a role for kinesin-2 in the translocation of arrestin into the outer segment. Part of this study demonstrated the light-dependent association of arrestin with mislocalized opsin in *Kif3a*-depleted rod photoreceptor cells. Therefore, we next tested whether light-dependent signaling from an opsin-arrestin complex was required for photoreceptor cell degeneration. These studies led to the demonstration of a clear relationship between the amount of opsin and the rate of photoreceptor cell death and loss, indicating the importance of mislocalized opsin in promoting photoreceptor cell degeneration.

MATERIALS AND METHODS

Mice

All procedures conformed to institutional animal care and use authorizations and were in accordance with regulations established by the National Institutes of Health. Mice were kept on a 12-h light/12-h dark cycle under 10–50 lux of fluorescent lighting during the light cycle. The genetic mutants used were *Kif3a*$^{flox/flox}$ (Marszalek *et al*., 2000), *RHO-Cre* (line 8) (Jimeno *et al*., 2006), arrestin (*Sag*) knockout (Xu *et al*., 1997), alpha-transducin (*Gnat1*) knockout (Calvert *et al*., 2000), and rod opsin (*Rho*) knockout (Lem *et al*., 1999) mice. All mice had been backcrossed on to the C57BL/6HNsd (Harlan C57BL/6) genetic background, which is considered "wild-type" for the purposes of this study. Breeding strategies and genotyping of the individual mutations followed that described previously (Xu *et al*., 1997; Lem *et al*., 1999; Marszalek *et al*., 2000; Jimeno *et al*., 2006). *RHO-Cre*$^{+}$ mice always contained only one transgenic allele, and *RHO-Cre*$^{-}$ mice contained none. Breeders were checked every day for the birth of a litter during the previous night; the day a litter was first observed was regarded as postnatal day 0 (P0). Dark-reared mice were placed in total darkness on P0; they were handled thereafter using infrared light and infrared converting binoculars. For dark to light experiments (concerning the localization of arrestin), mice were kept in a dark room overnight and subjected to 600 lux for 15 min.

Microscopy

Eyes were enucleated and posterior eyecups were fixed by immersion. For conventional light and electron microscopy, eyecups were fixed in 2% glutaraldehyde + 2% paraformaldehyde in 0.1 M cacodylate buffer, followed by secondary fixation in 1% OsO4 and processing for embedment in Epon. Photoreceptor cell density was determined from images of dorso-ventral semithin (0.7 μm) sections, stained with toluidine blue or Azure II. Regions that were spaced at 0.5-mm intervals from the optic nerve head were identified; the central retina corresponds approximately with the region that is 0.5 mm dorsal to the optic nerve head. In each region, at least three representative columns of photoreceptor cell nuclei were counted to determine the thickness of the nuclear layer in terms of the number of rows of nuclei.

For immunoelectron microscopy, eyecups were fixed in 0.25% glutaraldehyde + 4% formaldehyde in 0.1 M cacodylate buffer, pH 7.4, and processed for embedment in LR White. Ultrathin sections (70 nm) were etched with saturated sodium periodate for 15 min, blocked with 4% BSA in antibody buffer (TBS + 1% Tween-20) for 1 h at room temperature and incubated with rod opsin antibody (1D4) in buffer overnight at 4°C. Sections were then washed and incubated with goat anti-mouse IgG conjugated to 12 nm gold (Jackson Lab) and stained with uranyl acetate and lead citrate. Sections from rhodopsin knockout mice were used as negative control. Immunolabeling density was determined by counting gold particles over the inner segment plasma membrane (defined as a 60-nm band, centered on the center of the membrane), and over the area enclosed by this membrane (designated as *within* the inner segment).

For immunofluorescence microscopy, eyes were fixed in 4% paraformaldehyde in PBS. Eyecups were washed in PBS and subjected to dehydration in ethanol and xylene. Samples were embedded in paraffin. Sections (5 μm) were mounted on glass slides. Before staining with antibodies, samples were rehydrated and blocked in 4% BSA in PBS. Autofluorescence was quenched with 50 mM ammonium chloride in phosphate-buffered saline (PBS). Antibodies were diluted into Antibody Buffer (AB; 2% goat serum and 0.01% Triton X-100 in PBS). Sections were incubated with primary antibody solutions overnight at 4°C and secondary antibody for 1 h at room temperature in the dark. Sections were mounted using anti-fading mounting media containing DAPI (Fluorogel II, EMS, USA) and analyzed on an Olympus FluoView 1000 confocal microscope. The antibodies used were as follows: 1D4 (mouse monoclonal anti-opsin), R7 (rat polyclonal anti-arrestin), anti-caspase 3 active form (rabbit polyclonal, Millipore, Bedford, MA), and anti-phospho-c-jun (Ser63) II (rabbit polyclonal, Cell Signaling). The secondary antibodies used were Alexa 568 or Alexa 488 goat anti-rabbit, goat anti-rat, or goat anti-mouse IgG (Molecular Probes, Eugene, OR).

Western Blot Analysis

Mouse eyecups were homogenized in lysis buffer [50 mM Tris, pH 7.4, 100 mM NaCl, 1 mM EDTA, 1 mM $MgCl_2$, 1 mM DTT and complete protease inhibitor cocktail (Sigma, St. Louis, MO)]. Equivalent amounts of sample were fractionated on a 4–12% Bis-Tris gel (Invitrogen, Carlsbad, CA) and transferred to PVDF membrane (Millipore). Membranes were blocked in PBS/0.05% Tween-20 with 4% BSA (blocking solution). The membrane was then probed with anti-opsin, pAb01 (1:10,000), in blocking solution, washed four times in PBS/0.05% Tween, and incubated with horseradish peroxidase-conjugated anti-rabbit antibody (1:30,000, Sigma). Bound antibody was detected using the ECL Dura Western Blotting detection system (Amersham, Piscataway, NJ).

The chemilumiscence signal detected was used to perform densitometry analysis in ImageJ, where the intensity was correlated with relative protein levels. Samples were analyzed in triplicate.

TUNEL Labeling

Detection of apoptotic nuclei by TUNEL was performed using the TACS TdT Kit (R&D Systems, Minneapolis, MN) according to the manufacturer's protocol. Briefly, the paraffin was removed from paraffin-embedded sections, which were then hydrated, followed by permeabilization with proteinase K. Sections were then subjected to quenching of endogenous peroxidase with

Quenching Solution, and labeled with TdT for 1 h at 37 degrees. The labeling reaction was terminated with Stop Buffer. Detection was performed by incubation with streptavidin-HRP followed by diaminobenzidine (DAB) solution. Samples were analyzed on an Olympus FluoView 1000 confocal microscope. Positive and negative controls were used for the assay. As a positive control, a section of a WT retina was treated like the other sections, with the exception that before the quenching step, it was subjected to treatment with TACS-nuclease, to generate DNA breakage in most cells. As a negative control, a section of a WT retina was not labeled with the TdT labeling reaction mix. Quantification of the nuclei was performed using Image J software. Three different complete dorso-ventral sections per genotype were used. Because the negative controls showed no staining, stained (dark) nuclei were regarded as TUNEL-positive.

Electroretinographic Analysis

After overnight dark-adaptation, mice were anesthetized with an intraperitoneal injection of normal saline solution containing ketamine (15 μg/g) and xylazine (3 μg/g body weight). ERGs were recorded from the corneal surface of the eye after pupil dilation (1% atropine sulfate) using a gold loop corneal electrode together with a mouth reference and tail ground electrode. A drop of methylcellulose (2.5%), placed on the corneal surface, ensured electrical contact and corneal integrity. Responses were amplified (Grass CP511 AC amplifier, ×10,000; 3 dB down at 2 and 10,000 Hz) and digitized using an I/O board (National Instruments, PCI-1200) in a personal computer. Signal processing was performed with custom software (National Instruments, LabWindows/CVI). Mouse body temperature was maintained at a constant 38°C using a heated water pad.

All stimuli were presented in a large Ganzfeld dome (LKC Technologies), the interior surface painted with a highly reflective white matte paint (Eastman Kodak Corporation, #6080). Flash sequence and presentation frequency were under precise computer control. Rod-photoreceptor mediated ERGs were recorded to blue (Kodak Wratten 47A) light flashes over the range −4.67 to −0.44 log cd-s/m^2. Cone-photoreceptor mediated ERGs were recorded to white flashes (−0.54 to 0.70 log cd-s/m^2) superimposed on a rod-saturating background (32 cd/m^2) following 10 min of light adaptation.

RESULTS

Opsin Mislocalization in KIF3A-Depleted Photoreceptor Cells

Opsin mislocalization has been demonstrated by immunocytochemistry of KIF3A- or IFT-mutant photoreceptor cells (Marszalek *et al*., 2000; Pazour *et al*., 2002; Jimeno *et al*., 2006; Krock and Perkins, 2008; Avasthi *et al*., 2009; Sukumaran and Perkins, 2009). It is especially evident in mutant cone photoreceptor cells (Avasthi *et al*., 2009). The most obvious site of mislocalization is in the plasma membrane of the inner segment (Figure 1D) and nuclear layer (Supplemental Figure 1). However, there is also evidence of opsin within the inner segment of KIF3A-depleted photoreceptor cells (Marszalek *et al*., 2000; Jimeno *et al*., 2006). Here we quantified opsin immunogold labeling as a measure of opsin associated with intracellular and plasma membrane regions of the inner segments of *RHO-Cre*$^+$;*Kif3a*$^{flox/flox}$ rod photoreceptors at postnatal day 7 (P7), when opsin mislocalization can first be detected, and, a week later, at P14. The use of this *RHO-Cre* transgene results in synchronous excision of *Kif3a*^{flox} across the entire neonatal retina (Jimeno *et al*., 2006).

In P7 rod photoreceptors, the concentration of opsin labeling of the inner segment plasma membrane is similar between mutant and WT, but the amount of opsin labeling within the inner segment is significantly greater in mutant retinas (Figure 1). The overall amount of opsin in mutant and WT retinas is similar (Figure 1G), indicating that the additional opsin within the inner segment of mutant cells must be countered by less outer segment opsin. In P14 rod photoreceptors, there is still more opsin labeling within the inner segment of mutant compared with WT cells, but the striking difference is in the amount of opsin labeling associated with the plasma membrane of the inner segments, with 16-fold more in mutant retinas (Figure 1). These observations suggest that, in KIF3A-depleted rod photoreceptors, opsin is first backlogged along the intracellular trafficking route to the outer segment, then it accumulates in the plasma membrane outside of the outer segment. It is important to note that each KIF3A-depleted rod photoreceptor possesses a partly-developed outer segment [Figure 2B; see also Figure 5H in Jimeno *et al.* (2006) for immuno EM].

Arrestin Translocation in KIF3A-Depleted Photoreceptor Cells

In P14 *RHO-Cre*$^+$;*Kif3a*$^{flox/flox}$ retinas, opsin mislocalization is evident by immunofluorescence and rod photoreceptor cell loss has only just begun (cf. Figure 2B with A) (Jimeno *et al*., 2006). We therefore chose this time-point to study the effect of kinesin-2 function on the localization of arrestin in light- and dark-adapted retinas by immunofluorescence.

As described previously (reviewed in Strissel *et al*., 2006), arrestin normally migrates to the outer segment in the light, so that its concentration in the inner segment and nuclear layers of WT retinas is much greater in the dark than in the light (cf. Figure 2, G and H with 2, C and D). In KIF3A-depleted photoreceptors, arrestin remained in the inner segment and nuclear layers in both the light and dark (Figure 2, E and I). This observation is consistent with transport of arrestin by kinesin-2; however, on closer examination, it was clear that most of the arrestin becomes colocalized with mislocalized opsin in the light (cf. Figure 2, F and J, including higher magnification images shown in F′ and J′, which illustrate an increased overlap of the opsin and arrestin immunolabeling in the light). Hence, it is plausible that arrestin is simply prevented from migrating to the outer segment due to binding mislocalized photoactivated rhodopsin. In any case, it is important to note for subsequent parts of the current study, that light exposure appears to promote the formation of opsin–arrestin complexes in the inner segment and nuclear layers of KIF3A-depleted photoreceptors.

Test for Requirement of Arrestin and Light in Eliciting Photoreceptor Cell Loss

To test whether complexes of mislocalized rhodopsin and arrestin were required for the photoreceptor cell loss, we examined retinas from P21 *RHO-Cre*$^+$;*Kif3a*$^{flox/flox}$ mice that also lacked arrestin (*Sag*$^{-/-}$). Further, to eliminate photoactivation of rhodopsin and the phototransductive cascade, we reared animals in darkness. P21 was the most appropriate age to sample, because the steepest decline in *RHO-Cre*$^+$;*Kif3a*$^{flox/flox}$ photoreceptor cell number occurs during the third postnatal week (Jimeno *et al*., 2006).

RHO-Cre$^+$;*Kif3a*$^{flox/flox}$ mice showed severe photoreceptor cell loss by P21, with only 1–2 rows of photoreceptor cell nuclei evident in the central retina. Many of the remaining nuclei are from cones (containing multiple small clumps of heterochromatin) or rods that appear to be apoptotic (Figure 3). Dark rearing had no effect on this loss of cells, nor did lack of arrestin (Sag) stem this loss, because *RHO-Cre*$^+$;*Kif3a*$^{flox/flox}$;*Sag*$^{-/-}$ retinas and *RHO-Cre*$^+$;*Kif3a*$^{flox/flox}$ retinas from animals, reared in normal lighting or in darkness, all showed a similar degree of photoreceptor degeneration (Figure 3). Note that, although the *RHO-Cre*$^+$ transgene has been reported to effect retinal degeneration by itself, presumably due to Cre toxicity, degeneration is not evident until P49, with P28 animals showing no histological or electrophysiological defects (Jimeno *et al*., 2006).

Activation of the phototransductive cascade was also prevented by generating mice that lacked alpha transdu-

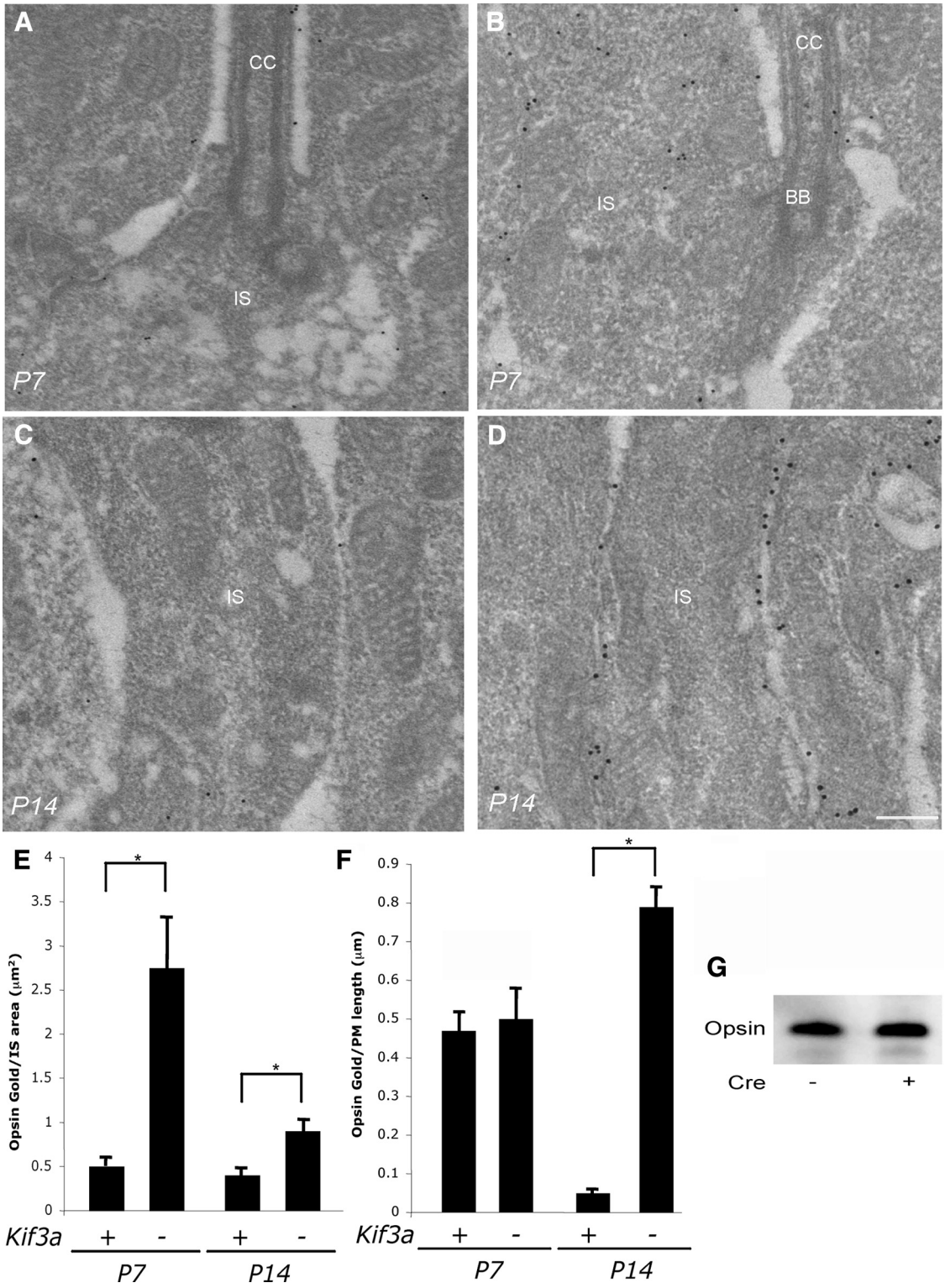

Figure 1. ImmunoEM of opsin in the inner segment at P7 and P14. Electron micrographs of opsin immunogold labeled sections from wild-type (A and C) and *RHO-Cre*$^{+}$*;Kif3a*$^{flox/flox}$ (B and D) mice at P7 (A and B) and P14 (C and D). IS, rod inner segment; BB, basal body; CC, connecting cilium. Scale bar = 200 nm; all panels same magnification. Bar graphs, illustrating the density of opsin immunogold labeling within the inner segment (E) and along the inner segment plasma membrane (F) of rod photoreceptors, in relation to the genotype and age. Error bars represent ± SEM, where n = 3 eyes. Asterisks indicate $p < 0.005$, by Student's one-tail, *t* test. (G) Western blot analysis of rod opsin in P7 WT (labeled as *Cre*$^{-}$) and *RHO-Cre*$^{+}$*;Kif3a*$^{flox/flox}$ (labeled as *Cre*$^{+}$) eyecups, illustrating the same amount of opsin of the same mobility, despite depletion of KIF3A.

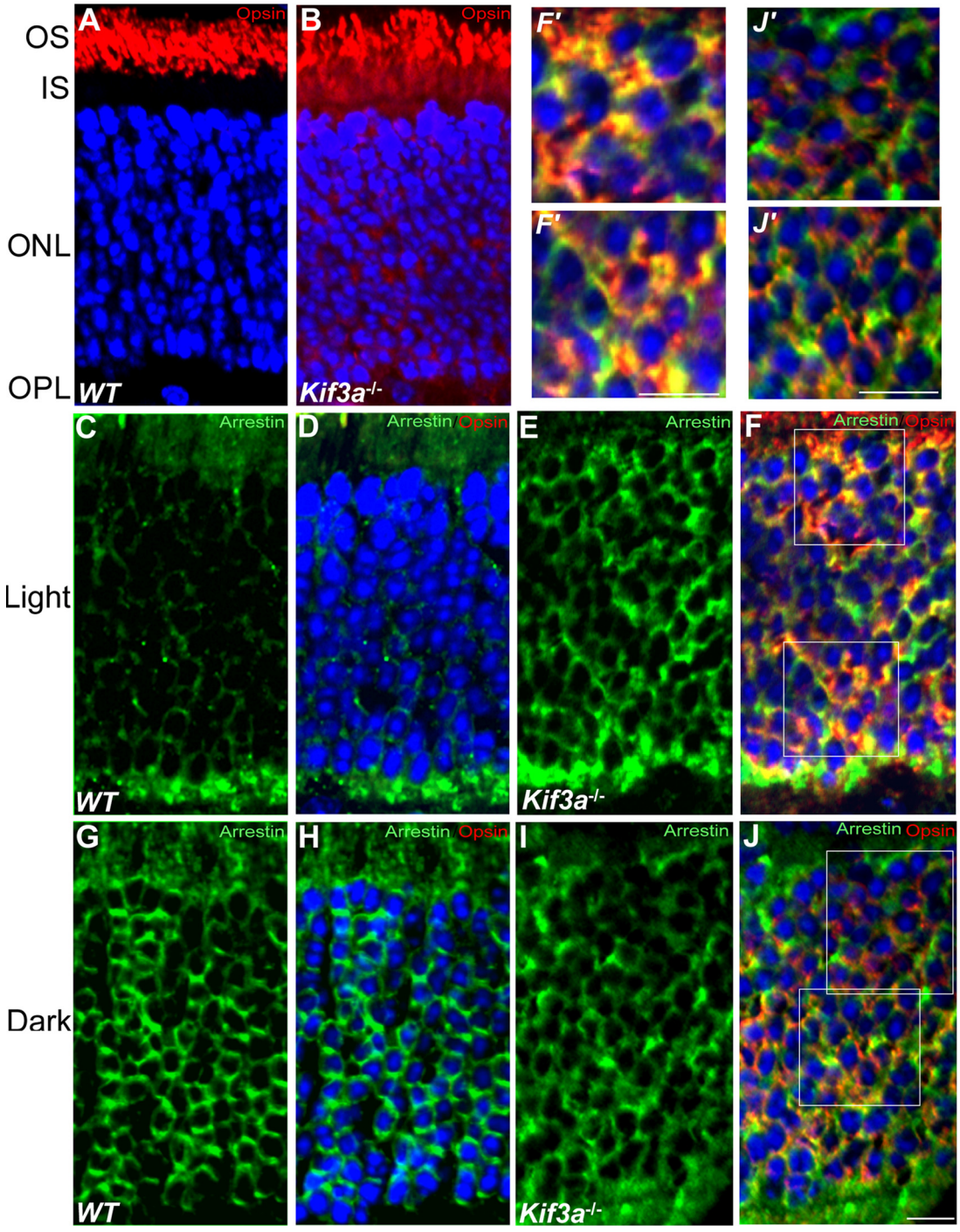

Figure 2. Arrestin translocation in KIF3A-depleted rod photoreceptor cells. Paraffin sections (5 μm) of retinas from wild-type (WT) and *RHO-Cre*$^{+}$;*Kif3a*$^{flox/flox}$ (labeled as *Kif3a*$^{-/-}$) mice at P14. (A and B) Retinas labeled with anti-opsin (red) and DAPI (blue). Loss of KIF3A results in the abnormal accumulation of opsin in the IS and ONL (B). (C–J) Sections from dark and light adapted animals labeled with arrestin antibodies (green). Panels D, F, H, and J also show labeling with opsin antibodies (red) and with DAPI (blue), although no opsin is evident in D and H, because it is not mislocalized in these WT retinas. Yellow represents overlap between opsin and arrestin labeling. (C–F) After exposure to light, following the dark adaptation. (G–J) After the dark adaptation, before light exposure. (F′, J′) Higher magnification of the ONL region of the mutant retinas (areas magnified are outlined in F and J). There is a greater overlap of arrestin and mislocalized opsin in the light (F) than in the dark (J). Scale bars = 10 μm. OS, outer segment layer; IS, inner segment layer; ONL, outer nuclear layer; OPL, outer plexiform layer.

cin (*Gnat1*). The extent of photoreceptor cell loss in retinas from P21 *RHO-Cre*$^{+}$;*Kif3a*$^{flox/flox}$;*Gnat1*$^{-/-}$ mice was similar to that in retinas from P21 *RHO-Cre*$^{+}$;*Kif3a*$^{flox/flox}$ mice (Supplemental Figure 2), supporting the result obtained from rearing the mice in the dark. Photoreceptor cell degeneration due to loss of kinesin-2 function therefore does not require signaling from an opsin-arrestin complex, activation of normal phototransduction, or any photoactivation of rhodopsin.

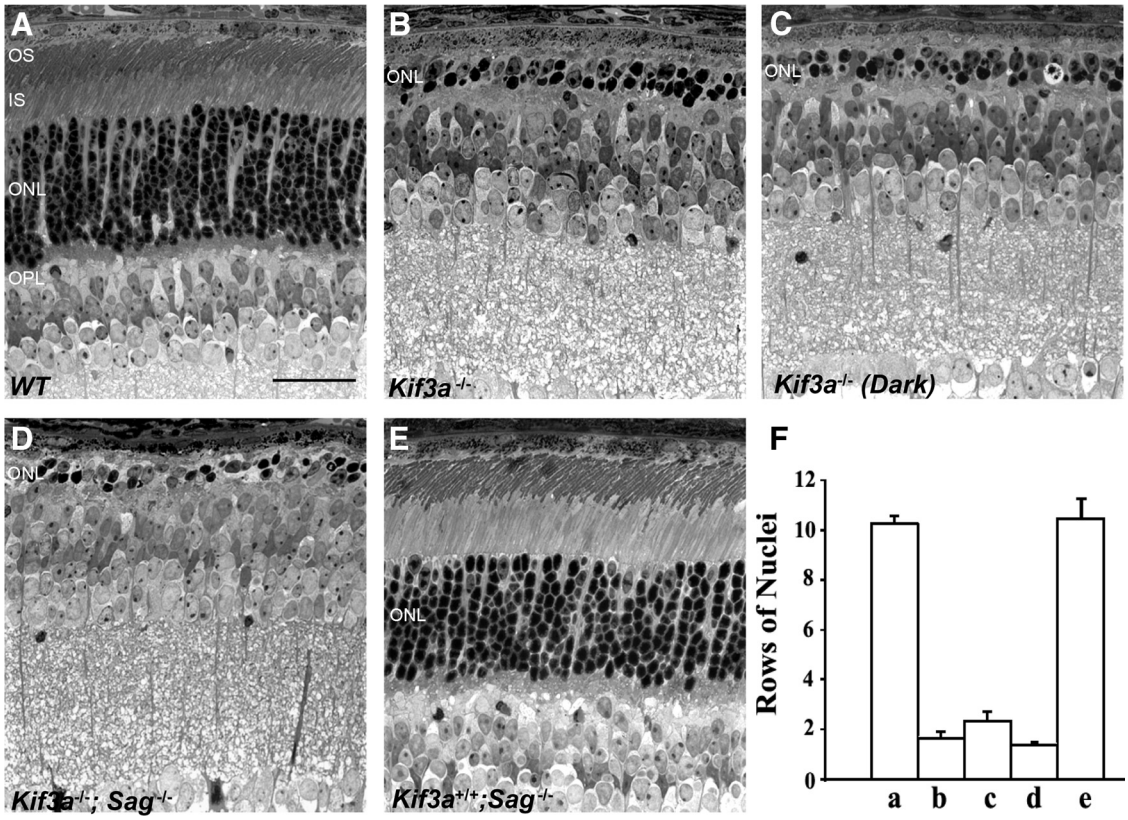

Figure 3. Loss of KIF3A-depleted rod photoreceptors in mice maintained in the dark or lacking arrestin. LM sections of photoreceptor cells in the region 0.5 mm dorsal to the optic nerve head, illustrating the extent of the photoreceptor cell nuclear layer in 21-d old mice that were (A) WT, (B) *RHO-Cre*$^{+}$;*Kif3a*$^{flox/flox}$ (i.e., lacking KIF3A), (C) *RHO-Cre*$^{+}$;*Kif3a*$^{flox/flox}$, (i.e., lacking KIF3A, reared in constant darkness), (D) *RHO-Cre*$^{+}$;*Kif3a*$^{flox/flox}$;*Sag*$^{-/-}$ (i.e., lacking both arrestin and KIF3A), or (E) *RHO-Cre*$^{-}$;*Kif3a*$^{flox/flox}$;*Sag*$^{-/-}$ (i.e., lacking arrestin, but with normal KIF3A, due to lack of Cre). On the images, *RHO-Cre*$^{+}$;*Kif3a*$^{flox/flox}$ has been indicated by *Kif3a*$^{-/-}$ and *RHO-Cre*$^{-}$;*Kif3a*$^{flox/flox}$ by *Kif3a*$^{+/+}$. All images were taken near the center of the retina, 0.5 mm dorsal from the optic nerve head. Except for C, all animals were reared under the normal light/dark cycle. All LMs are of the same magnification; scale bar = 50 μm. OS, outer segment layer; IS, inner segment layer; ONL, photoreceptor nuclear layer; OPL, photoreceptor synaptic layer. (F) Bar graph showing the counts of photoreceptor cells in relation to the different genotypes and lighting conditions; a–e correspond to the genotypes shown in A–E, respectively. The depth of the photoreceptor cell nuclear layer, in the region 0.5 mm dorsal to the optic nerve head, is expressed in terms of the number of rows of nuclei that span the layer (indicated as "ONL" in the micrographs). Error bars indicate SEM, where n > 3 animals for each genotype or condition. Neither light nor arrestin is required for photoreceptor degeneration due to loss of KIF3A.

Test for Requirement of Rod Opsin in Eliciting Photoreceptor Cell Loss

In the next set of experiments, we tested whether decreasing the expression of rhodopsin would affect the rate of photoreceptor cell loss. For the first month of life, retinas from heterozygous *Rho* knockout (*Rho*$^{+/-}$) mice contain the same number of photoreceptor cells as retinas of control (*Rho*$^{+/+}$) mice, although the individual rod photoreceptors contain only ~70% of the amount of rhodopsin present in control mice (Figure 4) (Lem *et al*., 1999). Despite the reduced opsin levels, mislocalized opsin is still evident after the depletion of KIF3A (Supplemental Figure 3). In comparing control, *RHO-Cre*$^{+}$;*Kif3a*$^{flox/flox}$, and *RHO-Cre*$^{+}$;*Kif3a*$^{flox/flox}$;*Rho*$^{+/-}$ retinas from P21 mice, we found that the presence of a single *Rho*$^{-}$ allele, and thus reduced rhodopsin content, resulted in significant, although incomplete rescue of photoreceptor cells (Figure 5, A–C). *RHO-Cre*$^{+}$;*Kif3a*$^{flox/flox}$;*Rho*$^{+/-}$ retinas had approximately three times as many photoreceptor cells across the retina as did *RHO-Cre*$^{+}$;*Kif3a*$^{flox/flox}$ retinas (Figure 5K).

By P28, all rod photoreceptor cells have been lost from *RHO-Cre*$^{+}$;*Kif3a*$^{flox/flox}$ retinas; the only remaining photoreceptor cell nuclei are from cone photoreceptor cells, which form a single row of cell nuclei (Figure 5G) (cf. Jimeno *et al*., 2006). *RHO-Cre*$^{+}$;*Kif3a*$^{flox/flox}$;*Rho*$^{+/-}$ retinas from P28 mice were also severely degenerate, although they contained ~3 rows of photoreceptor cell nuclei, indicating that a significant number of rod photoreceptor cells still survived, and the rescue effect of *Rho*$^{+/-}$ was still evident (Figure 5H).

Rho$^{-/-}$ mouse retinas do not contain detectable rod opsin (Figure 4) (Lem *et al*., 1999). We therefore tested whether the complete absence of rod opsin would inhibit photoreceptor cell loss further. This proved to be the case. At both P21 and P28, *RHO-Cre*$^{+}$;*Kif3a*$^{flox/flox}$;*Rho*$^{-/-}$ mice have significantly more photoreceptor cells remaining than *RHO-Cre*$^{+}$;*Kif3a*$^{flox/flox}$;*Rho*$^{+/-}$ mice (Figure 5, D and I). This additional rescue is despite some photoreceptor cell loss due to the lack of RHO alone (Lem *et al*., 1999) (Figure 5E and J). Indeed, the contribution of KIF3A depletion to photoreceptor cell loss in *Rho*$^{-/-}$ mice was found to be only minor, and counts taken from some regions of P21, P28, and P35 mice indicated no significant effect of KIF3A depletion (Figure 5, K–M).

Figure 5M shows time course plots of photoreceptor cell death with different expression levels of opsin. The effect of reducing opsin by ~30% (as in *Rho*$^{+/-}$ mice) results in a

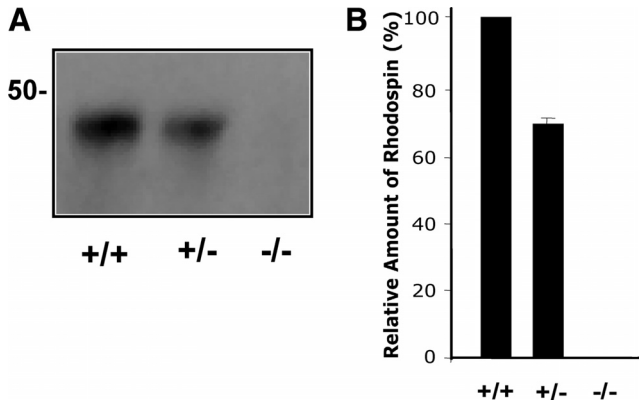

Figure 4. Rhodopsin levels in retinas of mice, with two (WT, +/+), one (heterozygote, +/−), or no (null, −/−) functional *Rho* genes. (A) Western blot analysis of rhodopsin levels in $Rho^{+/+}$, $Rho^{+/-}$, and $Rho^{-/-}$ mice. An equivalent portion of eyecup lysate was loaded for each genotype. The position of a 50-kDa molecular mass marker is shown on the left. (B) Bar graph showing the relative amount of rhodopsin in $Rho^{+/+}$, $Rho^{+/-}$, and $Rho^{-/-}$ eyes, measured from Western blots, such as that shown in A, by densitometry, and expressed as a percentage of that in $Rho^{+/+}$ eyes. Loss of one copy of the rhodopsin gene results in a 28% reduction in opsin levels. Error bars represent ± SEM, where n = 3 animals.

delay in photoreceptor cell loss of approximately one week. Elimination of opsin results in a larger delay, although this time course becomes confounded by the degenerative effect of $Rho^{-/-}$. The presence of the *RHO-Cre* transgene also eventually causes photoreceptor cell loss, but none is detectable at P28 (Jimeno *et al*., 2006).

Test for Requirement of Rod Opsin in Eliciting Photoreceptor Cell Apoptosis

Previously, we showed that aberrant opsin localization in $IRBP\text{-}Cre^{+};Kif3a^{flox/flox}$ retinas was followed by the appearance of TUNEL-positive nuclei (Marszalek *et al*., 2000). Here, in addition to the TUNEL assay, which does not discriminate among autolytic, necrotic, and apoptotic cells (Grasl-Kraupp *et al*., 1995), we measured the presence of two more specific apoptotic indicators, immunofluorescence labeling with antibodies against c-Jun that is phosphorylated at Ser63 and with antibodies against activated caspase-3. We also counted condensed nuclei by electron microscopy. All four indicators were greatly increased in P14 $RHO\text{-}Cre^{+};Kif3a^{flox/flox}$ retinas compared with P14 retinas from WT mice or mice lacking the floxed *Kif3a* gene or *RHO-Cre*.

Next, we tested whether the protective effect of reduced opsin expression, in terms of inhibiting the loss of KIF3A-depleted rods, was due to inhibition of apoptosis, as determined by these four indicators. We studied retinas from P14 mice of different genotypes. By the TUNEL assay, 30% of the photoreceptor nuclei in $RHO\text{-}Cre^{+};Kif3a^{flox/flox}$ retinas were positive, approximately six times the number of positive nuclei in retinas that also lacked RHO (from $RHO\text{-}Cre^{+};Kif3a^{flox/flox};Rho^{-/-}$ mice) (Figure 6A). By electron microscopy, 20% of the photoreceptor nuclei appeared condensed in $RHO\text{-}Cre^{+};Kif3a^{flox/flox}$ retinas, whereas no condensed nuclei were observed in retinas that also lacked RHO (from $RHO\text{-}Cre^{+};Kif3a^{flox/flox};Rho^{-/-}$ mice) or did not contain $Kif3a^{flox/flox}$ (Figure 6B-D). Similarly, phospho-c-Jun (Figure 6E) and activated caspase-3 (Figure 6F) immunofluorescence was evident in $RHO\text{-}Cre^{+};Kif3a^{flox/flox}$ retinas, but negligible in retinas that lacked RHO or were wild-type for *Kif3a*. These results indicate that the loss of KIF3A-depleted rod photoreceptor cells is due to caspase-dependent apoptotic cell death, and that this pathway is triggered by the mislocalization of opsin.

ERG Measurements of Photoreceptor Function

To test whether the protective effect of reduced opsin expression in KIF3A-depleted rods was evident in terms of photoreceptor function as well as survival, we measured ERG responses in mice of different genotypes at P21 and at P35. At P21, rod photoreceptor-mediated responses had higher amplitudes in $RHO\text{-}Cre^{+};Kif3a^{flox/flox};Rho^{+/-}$ mice in comparison with $RHO\text{-}Cre^{+};Kif3a^{flox/flox}$ mice, indicating that the additional surviving rods, due to decreased RHO, are functional (Figure 7A). This increase in amplitude was evident despite reduced amplitudes in $Rho^{+/-}$ mice compared with WT mice. Cone-mediated responses were also greater in the $RHO\text{-}Cre^{+};Kif3a^{flox/flox}$mice with reduced ($Rho^{+/-}$) or no RHO than in $RHO\text{-}Cre^{+};Kif3a^{flox/flox}$ mice with $Rho^{+/+}$ (Figure 7C), indicating that the increased rod survival extends to increased cone function. At P35, cone responses in $RHO\text{-}Cre^{+};Kif3a^{flox/flox};Rho^{-/-}$ mice were clearly detectable, whereas we could not detect any cone responses in the $RHO\text{-}Cre^{+};Kif3a^{flox/flox}$ mice with $Rho^{+/+}$ (Figure 7D). Nevertheless, the cone responses from retinas of $RHO\text{-}Cre^{+};Kif3a^{flox/flox};Rho^{-/-}$ mice were significantly smaller than those in the $Rho^{-/-}$ mice. Together these ERG measurements show that the increased photoreceptor survival due to reduction of RHO in KIF3A-depleted rod photoreceptors also results in increased rod and cone responsiveness.

DISCUSSION

Here, we have explored further the role of kinesin-2 in rod photoreceptor cells and in particular the basis of the very rapid photoreceptor cell loss that follows the loss the kinesin-2 function. We report that arrestin fails to translocate to the outer segment upon light exposure in KIF3A-depleted rods; it instead associates with mislocalized opsin. However, unlike in a number of other models of photoreceptor degeneration, signaling from opsin–arrestin complexes is not required for cell death. Indeed, light-activation of rhodopsin is not even required. Our results indicate that the critical event is simply mislocalization of opsin, which, as we show, accumulates in large amounts first within the inner segment and then in the plasma membrane of the inner segment and nuclear region. Reduction in the expression of opsin in KIF3A-depleted rods markedly inhibits apoptosis and photoreceptor cell loss, and preserves photoreceptor function.

Protein traffic along the photoreceptor cilium is extremely busy, thus representing an extraordinary example of IFT. Ten percent of the opsin-containing disk membranes of the outer segment in mammalian rods are renewed each day (Besharse and Hollyfield, 1979). The mislocalization of opsin that occurs in response to loss of function of kinesin-2 or IFT88 (Marszalek *et al*., 2000; Pazour *et al*., 2002; Jimeno *et al*., 2006) suggests that IFT powers the delivery of at least this protein. Opsin is the most abundant protein of the outer segment (Papermaster *et al*., 1975), at $\sim 7 \times 10^7$ molecules per mouse rod (Lyubarsky *et al*., 2004). Nevertheless, arrestin is also very highly concentrated in rod photoreceptor cells, with about one molecule for every 1.3 molecules of opsin (Strissel *et al*., 2006). Given that the majority of arrestin (and other soluble signaling proteins, transducin and recoverin) translocates between the inner and outer segment at every light-dark transition (Broekhuyse *et al*., 1985; Strissel *et al*., 2004), the trafficking of soluble signaling proteins involves

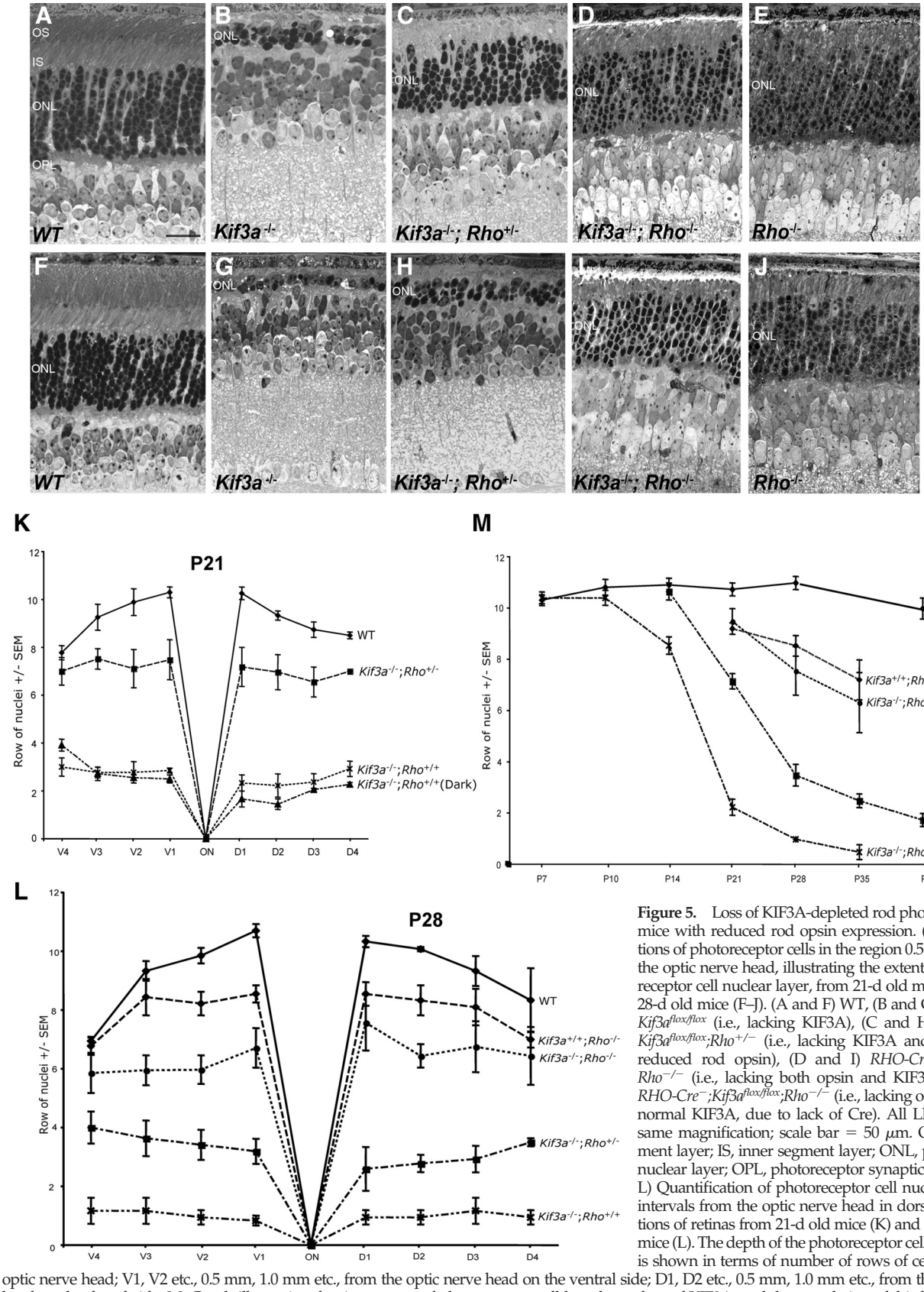

Figure 5. Loss of KIF3A-depleted rod photoreceptors in mice with reduced rod opsin expression. (A–J) LM sections of photoreceptor cells in the region 0.5 mm dorsal to the optic nerve head, illustrating the extent of the photoreceptor cell nuclear layer, from 21-d old mice (A–E) and 28-d old mice (F–J). (A and F) WT, (B and G) *RHO-Cre*$^{+}$;*Kif3a*$^{flox/flox}$ (i.e., lacking KIF3A), (C and H) *RHO-Cre*$^{+}$;*Kif3a*$^{flox/flox}$;*Rho*$^{+/-}$ (i.e., lacking KIF3A and with ~30% reduced rod opsin), (D and I) *RHO-Cre*$^{+}$;*Kif3a*$^{flox/flox}$;*Rho*$^{-/-}$ (i.e., lacking both opsin and KIF3A), (E and J) *RHO-Cre*$^{-}$;*Kif3a*$^{flox/flox}$;*Rho*$^{-/-}$ (i.e., lacking opsin, but with normal KIF3A, due to lack of Cre). All LMs are of the same magnification; scale bar = 50 μm. OS, outer segment layer; IS, inner segment layer; ONL, photoreceptor nuclear layer; OPL, photoreceptor synaptic layer. (K and L) Quantification of photoreceptor cell nuclei at 0.5-mm intervals from the optic nerve head in dorso-ventral sections of retinas from 21-d old mice (K) and from 28-d old mice (L). The depth of the photoreceptor cell nuclear layer is shown in terms of number of rows of cell nuclei. ON, optic nerve head; V1, V2 etc., 0.5 mm, 1.0 mm etc., from the optic nerve head on the ventral side; D1, D2 etc., 0.5 mm, 1.0 mm etc., from the optic nerve head on the dorsal side. M, Graph illustrating the time course of photoreceptor cell loss due to loss of KIF3A, and the retardation of this loss when rod opsin is reduced. The number of rows of the photoreceptor cell nuclei, in the region 0.5 mm dorsal to the optic nerve head, is shown. In K and L, error bars indicate ± SEM, where n > 3 animals for each genotype or condition. In all panels, *RHO-Cre*$^{+}$;*Kif3a*$^{flox/flox}$ has been indicated by *Kif3a*$^{-/-}$ and *RHO-Cre*$^{-}$;*Kif3a*$^{flox/flox}$ by *Kif3a*$^{+/+}$.

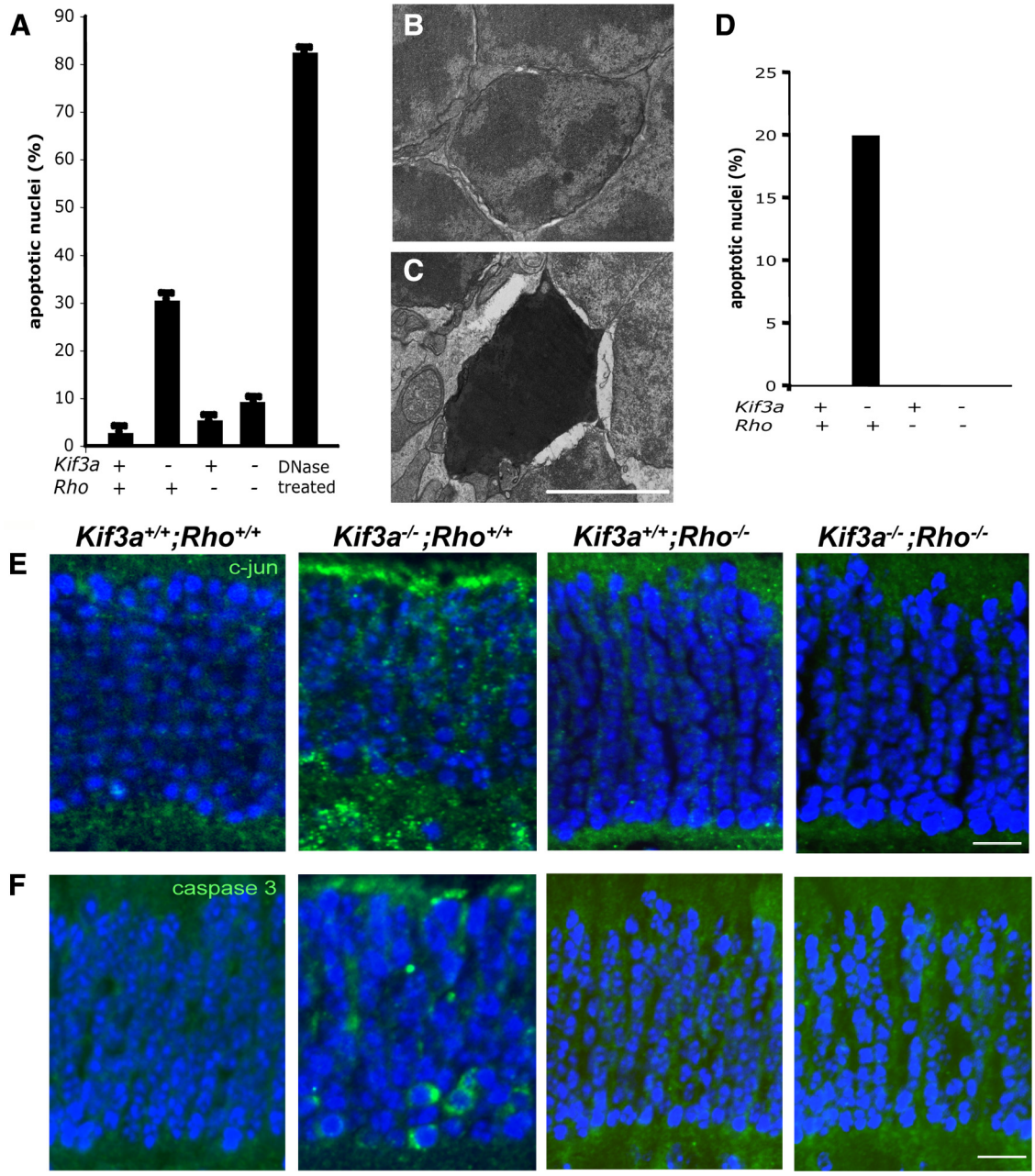

Figure 6. Apoptosis in relation to rod opsin expression. (A) Bar graph illustrating counts of apoptotic photoreceptor nuclei detected by a positive reaction in the TUNEL assay. (B and C) Electron micrographs of ultrathin sections (70 nm) of retinas from WT (A) and *RHO-Cre*$^{+}$*;Kif3a*$^{flox/flox}$ (B) mice at P14. Scale bar = 0.5 μm. A typical condensed apoptotic nucleus is shown in C. Such nuclei were scored as apoptotic for the bar graph shown in D. (D) Bar graph illustrating counts of apoptotic nuclei detected by condensed nuclei in electron micrographs. Only *RHO-Cre*$^{+}$*;Kif3a*$^{flox/flox}$ animals (i.e., *Kif3a*$^{-/-}$ and *Rho*$^{+/+}$) had apoptotic nuclei detectable by electron microscopy. Error bars indicate ± SEM, where n > 3 animals for each genotype or condition. (E and F) Paraffin sections (5 μm) of retinas labeled with antibodies against phosphorylated (Ser63) c-Jun (E) or against cleaved (activated) caspase 3 (F), shown in green, and with DAPI (blue). Scale bar = 15 μm. Mice contained rod photoreceptors that were either homozygous WT (+) or homozygous null (−) for *Kif3a* and *Rho*. Error bars indicate ± SEM, where n > 3 animals for each genotype or condition.

orders of magnitude more ciliary traffic than opsin and other disk membrane proteins. So, if IFT were responsible for the movement of these soluble signaling proteins, this would be, by far, its major task. Calvert *et al.* argued that diffusion could account for the delivery of arrestin and transducin to the outer segment (Calvert *et al.*, 2006). Our results are consistent with their argument. Although arrestin is mislocalized in light-adapted KIF3A-depleted rods, our results suggest that this defect could be a result of binding to mislocalized rhodopsin, and so do not necessarily indicate that kinesin-2 transports arrestin.

The mislocalization of opsin observed in the first studies of genetic disruption of kinesin-2/IFT was taken as evidence that opsin is transported by kinesin-2/IFT along the photoreceptor cilium (Marszalek *et al.*, 2000; Pazour *et al.*, 2002). More recently, this suggestion has been questioned for rods,

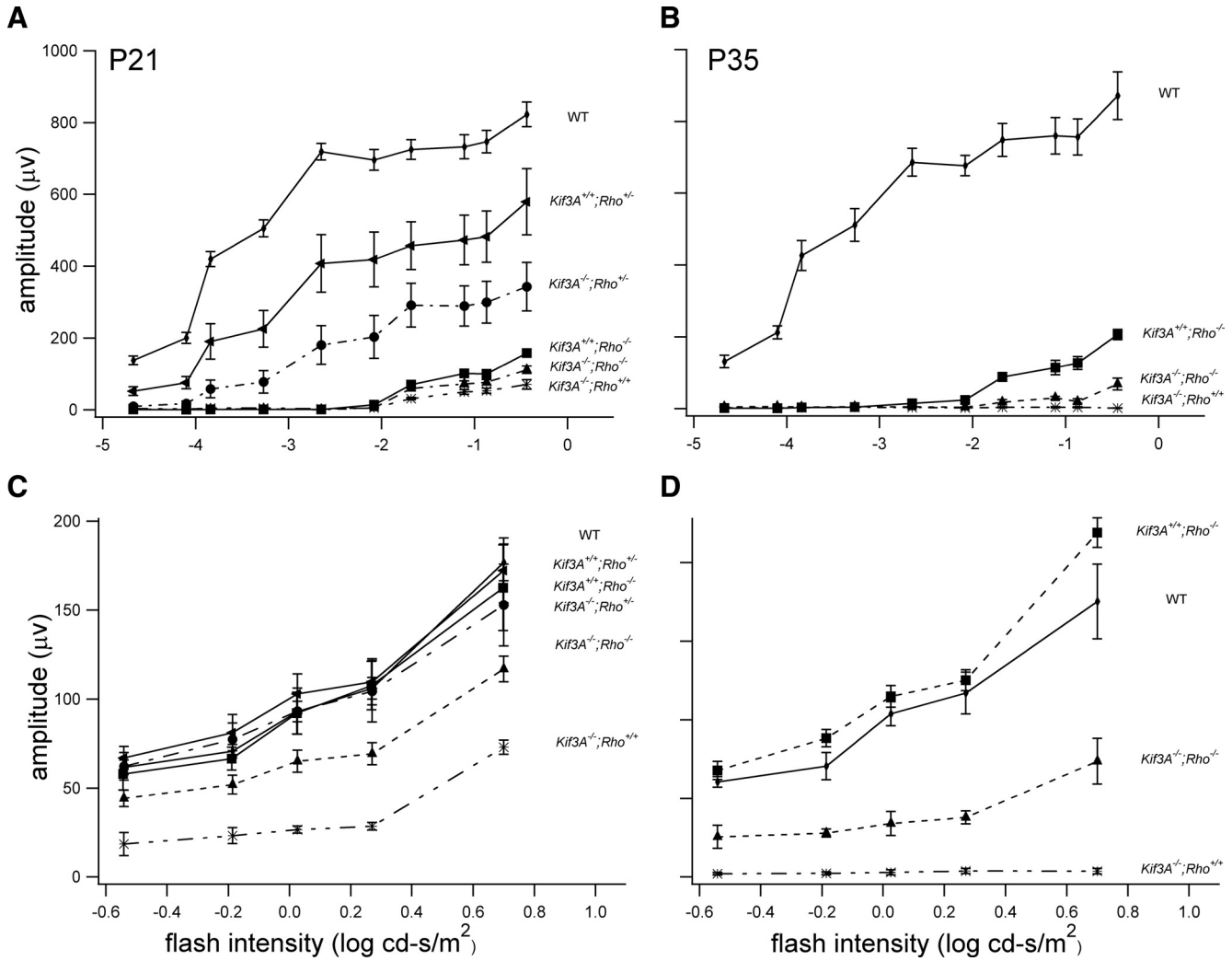

Figure 7. Intensity-response functions for dark- (A and B) and light- (C and D) adapted retinas. ERG responses were recorded at P21 (A and C) and at P35 (B and D). In A–D, *b*-wave amplitude, defined conventionally as the amplitude from the trough of the *a*-wave to the peak of the *b*-wave, is plotted against increasing intensity. *RHO-Cre*$^{+}$*;Kif3a*$^{flox/flox}$ has been indicated by *Kif3a*$^{-/-}$ and *RHO-Cre*$^{-}$*;Kif3a*$^{flox/flox}$ by *Kif3a*$^{+/+}$. For the dark-adapted ERGs (A and B) responses obtained to intensities below about −1.5 log cd-s/m^2 are assumed to be mediated by rods, whereas responses to higher intensities, while rod-dominated, also mask a small contribution from cones (Nusinowitz *et al*., 2007). Thus, the small dark-adapted response at the highest intensities in Rho$^{-/-}$ mice likely reflects this residual cone signal. The light-adapted ERGs (C and D) are mediated by cones. Error bars indicate ± SEM.

because, in comparison to cones, the mislocalization of opsin (and other outer segment proteins) seemed relatively minor (Avasthi *et al*., 2009). However, the present results document quantitatively that a backlog of opsin occurs very early in KIF3A-depleted rods (at P7, long before any cell death) and that rod opsin expression is key to the death of these cells. Both these observations are consistent with a direct link between kinesin-2 function and normal delivery of opsin to the outer segment, as suggested in earlier reports.

The high concentration of rhodopsin in a rod photoreceptor cell provides exquisite light sensitivity, but this level is close to the maximum that the cell can tolerate. An increase in opsin levels by just ~23% is sufficient to induce photoreceptor cell degeneration (Tan *et al*., 2001). Our results indicate that aberrant accumulation of this highly abundant protein outside of the outer segment initiates cell death, and that the essential factor for apoptosis is the abundance of the protein, rather than its signaling properties as a G-protein coupled receptor. It is possible that the abnormal accumulation of other outer segment proteins may also promote cell death. However, the nearly complete negation of loss of KIF3A-depleted rods by *Rho*$^{-/-}$ indicates that the accumulation of opsin is a major initiator of cell death.

A variety of models of inherited photoreceptor degeneration, such as *rd1* and *rds* mice and the *RCS* rat, also demonstrate mislocalized opsin before cell death (Nir and Papermaster, 1986; Jansen *et al*., 1987; Nir *et al*., 1987; Usukura and Bok, 1987; Nir *et al*., 1989). However, the opsin in these examples appears to be restricted to the plasma membrane of the cell and is thus distinct from the excessive amount of opsin that accumulates initially within the inner segment, as a result of kinesin-2 dysfunction. It may represent redistribution from the outer segment, as a secondary response in ailing cells that are dying by a different mechanism. Interestingly, cell death in at least the *rd1* and *rds* mice may be largely caspase-independent (Doonan *et al*., 2005; Lohr *et al*., 2006). In contrast to the increased capase-3 activity we detected in P14 KIF3A-depleted photoreceptor cells, labeling of

active capase-3 was not detected in photoreceptor nuclei of P7–13 *rd1* retinas (Doonan *et al.*, 2005).

Different mutations in rod opsin have been shown to affect its delivery to the outer segment. Some of these mutations perturb the correct folding of the protein (Sung *et al.*, 1991; Chapple *et al.*, 2001). In cell culture, the P23H mutant opsin accumulates in aggresomes and is targeted to the proteasome system, which it impairs (Illing *et al.*, 2002). In transgenic mice, P23H mutant opsin accumulates in perinuclear regions, at least in the absence of wild-type rod opsin (Frederick *et al.*, 2001). However, there is no suggestion that the nontrafficked opsin in KIF3A-depleted photoreceptor cells is misfolded. The primary cellular effect of dysfunctional kinesin-2 in photoreceptor cells appears to be loss of transport along the cilium, with the accumulation of opsin in the inner segment, resulting from a backlog. Concanavalin A labels the accumulated opsin, indicating that it has been processed normally through the endoplasmic reticulum and Golgi apparatus (Marszalek *et al.*, 2000).

A second class of opsin mutants appears to have defective targeting to the outer segment, and are therefore more comparable to kinesin-2 dysfunction. An important factor in the targeting of opsin to the outer segment is the presence of a localization signal and protein binding sites in the C-terminal region of the protein (Deretic *et al.*, 1998; Tam *et al.*, 2000; Deretic *et al.*, 2005). Mutations in the C-terminal region of rod opsin result in defects in the targeting of opsin to the outer segment, although, interestingly, despite numerous reports on such models (e.g., Sung *et al.*, 1994; Li *et al.*, 1996; Green *et al.*, 2000; Concepcion *et al.*, 2002; Tam and Moritz, 2006), invariably, mislocalized opsin has been shown throughout the plasma membrane of the cell, with no significant opsin accumulation inside the cell. We demonstrate here that, with the dysfunction of a molecular motor, there is first a backlog of opsin along the route to the outer segment within the cell (Figure 1). This backlog occurs despite the presence of a partly-developed outer segment (Figure 2B, Suppl. Figure 3) (Jimeno *et al.*, 2006). Nevertheless, opsin C-terminal mutations appear to be similar to kinesin-2 dysfunction in that apoptosis does not appear to require normal opsin signaling, since retinal degeneration still proceeds under darkness (Green *et al.*, 2000; Tam and Moritz, 2006).

A third type of opsin mutation that poses an interesting contrast to our observations with depleted KIF3A is the constitutively active K296E opsin. As shown recently, this opsin is phosphorylated not just in the light, but also in the dark, and is mislocalized throughout the photoreceptor cell only in the presence of arrestin (Chen *et al.*, 2006). Chen *et al.* have argued that this mutant opsin forms a complex with arrestin to activate apoptosis, similar to that reported for some Drosophila retinal degenerations (Alloway *et al.*, 2000; Kiselev *et al.*, 2000).

In addition to kinesin-2 and IFT proteins, there has been recent interest in proteins that are associated with the connecting cilium, and whose function may be related to transport along this structure. Many of these proteins are associated with retinal degenerations, such as Bardet-Biedl syndrome (BBS proteins), Senior Loken syndrome (NPHP proteins), Leber's congenital amaurosis (CEP290/NPHP6), and X-linked retinitis pigmentosa (RPGR, RPGRIP). In mouse models of some of these diseases, opsin has been reported to be present throughout the photoreceptor cell membrane before retinal degeneration (Zhao *et al.*, 2003; Nishimura *et al.*, 2004; Chang *et al.*, 2006). In a closer examination of opsin distribution in *Ahi1*$^{-/-}$ mice, another ciliopathic model with photoreceptor cell loss, an abnormal accumulation of opsin was found also within the inner segment before cell death (Louie *et al.*, 2010). It seems likely that mislocalized opsin may be an important trigger for retinal degeneration in ciliopathies in general.

Because the ectopic opsin in KIF3A-depleted photoreceptor cells is not providing any necessary signal due to photoactivation or by forming a complex with arrestin, how does it activate apoptosis? Looking further afield, among neurodegenerations in general, there are clear examples of cellular catastrophe that ensues from blockage of transport. Huge accumulations of debris were demonstrated in axons of kinesin-mutant *Drosophila* (Hurd and Saxton, 1996). A variety of neurodegenerative diseases have since been linked to defects in axonal transport resulting from compromised molecular motor function (summarized in Perlson *et al.*, 2010). Examples include Amyotrophic Lateral Sclerosis (ALS) and Alzheimer's disease (AD). A cause of familial ALS is mutant *SOD1* (which encodes superoxide dismutase 1). Mutant *SOD1* in mice has a number of consequences, but one includes possible effects on dynein and impairment of retrograde transport in axons of motor neurons (Chevalier-Larsen and Holzbaur, 2006). Mutations in *APP* (which encodes amyloid precursor protein) have been associated with familial AD. The axonal transport of APP is mediated by direct binding to a light chain subunit of kinesin-1 (KLC1) (Kamal *et al.*, 2000). Lowering the expression level of KLC1 in *APP*-mutant mice promotes axonal swellings, containing accumulated cellular material, and increased amyloid deposition (Stokin *et al.*, 2005). A common theme in these neurodegenerative disorders is that a relatively specific trafficking defect progresses to have a general effect on axonal transport. The loss of kinesin-2 function in photoreceptor cells has a similar consequence; first, opsin and perhaps some other cotransported proteins accumulate, then the trafficking of other cellular components, which use alternative pathways but still travel to the outer segment (e.g., the protein, peripherin/rds), is affected. The sheer mass of the resulting backlog appears to be the critical factor, and backlogs in different neurodegenerations might thus elicit a similar path to cell death.

ACKNOWLEDGMENTS

We thank Drs. Janis Lem and Jeannie Chen for the gifts of *Rho*$^{-/-}$, *Gnat1*$^{-/-}$, and *Arr*$^{-/-}$ mice that were used for breeding in the present study. We are also grateful to Drs. Larry Goldstein and Eric Pierce for the *Kif3a*^{flox} and *RHO-Cre* mice, which were used in previous collaborative studies, and Dr. Bob Molday for the gift of opsin mAb, 1D4. We thank Drs. Larry Goldstein and Dan Gibbs for helpful discussions, and Karen Teofilo for technical assistance. This research was supported by National Institutes of Health grants (to D.S.W.). D.S.W. is a Jules and Doris Stein RBP Professor.

REFERENCES

Alfinito, P. D., and Townes-Anderson, E. (2002). Activation of mislocalized opsin kills rod cells: a novel mechanism for rod cell death in retinal disease. Proc. Natl. Acad. Sci. USA *99*, 5655–5660.

Alloway, P. G., Howard, L., and Dolph, P. J. (2000). The formation of stable rhodopsin-arrestin complexes induces apoptosis and photoreceptor cell degeneration. Neuron *28*, 129–138.

Avasthi, P., Watt, C. B., Williams, D. S., Le, Y. Z., Li, S., Chen, C. K., Marc, R. E., Frederick, J. M., and Baehr, W. (2009). Trafficking of membrane proteins to cone but not rod outer segments is dependent on heterotrimeric kinesin-II. J. Neurosci. *29*, 14287–14298.

Besharse, J. C., and Hollyfield, J. G. (1979). Turnover of mouse photoreceptor outer segments in constant light and darkness. Invest. Ophthalmol. Vis. Sci. *18*, 1019–1024.

Broekhuyse, R. M., Tolhuizen, E. F., Janssen, A. P., and Winkens, H. J. (1985). Light induced shift and binding of S-antigen in retinal rods. Curr. Eye Res. *4*, 613–618.

Calvert, P. D., Krasnoperova, N. V., Lyubarsky, A. L., Isayama, T., Nicolo, M., Kosaras, B., Wong, G., Gannon, K. S., Margolskee, R. F., Sidman, R. L., Pugh, E. N., Jr., Makino, C. L., and Lem, J. (2000). Phototransduction in transgenic mice after targeted deletion of the rod transducin alpha -subunit. Proc. Natl. Acad. Sci. USA *97*, 13913–13918.

Calvert, P.D., Strissel, K. J., Schiesser, W. E., Pugh, E. N., Jr., and Arshavsky, V. Y. (2006). Light-driven translocation of signaling proteins in vertebrate photoreceptors. Trends Cell Biol. *16*, 560–568.

Chang, B., Khanna, H., Hawes, N., Jimeno, D., He, S., Lillo, C., Parapuram, S. K., Cheng, H., Scott, A., Hurd, R. E., Sayer, J. A., Otto, E. A., Attanasio, M., O'Toole, J., F., Jin, G., Shou, C., Hildebrandt, F., Williams, D. S., Heckenlively, J. R., and Swaroop, A. (2006). In-frame deletion in a novel centrosomal/ciliary protein CEP290/NPHP6 perturbs its interaction with RPGR and results in early-onset retinal degeneration in the rd16 mouse. Hum. Mol. Genet. *15*, 1847–1857.

Chapple, J. P., Grayson, C., Hardcastle, A. J., Saliba, R. S., van der Spuy, J., and Cheetham, M. E. (2001). Unfolding retinal dystrophies: a role for molecular chaperones? Trends Mol. Med. *7*, 414–421.

Chen, J., Shi, G., Concepcion, F. A., Xie, G., Oprian, D., and Chen, J. (2006). Stable rhodopsin/arrestin complex leads to retinal degeneration in a transgenic mouse model of autosomal dominant retinitis pigmentosa. J. Neurosci. *26*, 11929–11937.

Chevalier-Larsen, E., and Holzbaur, E. L. (2006). Axonal transport and neurodegenerative disease. Biochim. Biophys. Acta *1762*, 1094–1108.

Concepcion, F., Mendez, A., and Chen, J. (2002). The carboxyl-terminal domain is essential for rhodopsin transport in rod photoreceptors. Vision Res. *42*, 417–426.

Deretic, D., Schmerl, S., Hargrave, P. A., Arendt, A., and McDowell, J. H. (1998). Regulation of sorting and post-Golgi trafficking of rhodopsin by its C-terminal sequence QVS(A)PA. Proc. Natl. Acad. Sci. USA *95*, 10620–10625.

Deretic, D., Williams, A. H., Ransom, N., Morel, V., Hargrave, P. A., and Arendt, A. (2005). Rhodopsin C terminus, the site of mutations causing retinal disease, regulates trafficking by binding to ADP-ribosylation factor 4 (ARF4). Proc. Natl. Acad. Sci. USA *102*, 3301–3306.

Doonan, F., Donovan, M., and Cotter, T. G. (2005). Activation of multiple pathways during photoreceptor apoptosis in the rd mouse. Invest Ophthalmol. Vis. Sci. *46*, 3530–3538.

Frederick, J. M., Krasnoperova, N. V., Hoffmann, K., Church-Kopish, J., Ruther, K., Howes, K., Lem, J., and Baehr, W. (2001). Mutant rhodopsin transgene expression on a null background. Invest. Ophthalmol. Vis. Sci. *42*, 826–833.

Grasl-Kraupp, B., Ruttkay-Nedecky, B., Koudelka, H., Bukowska, K., Bursch, W., and Schulte-Hermann, R. (1995). In situ detection of fragmented DNA (TUNEL assay) fails to discriminate among apoptosis, necrosis, and autolytic cell death: a cautionary note. Hepatology *21*, 1465–1468.

Green, E. S., Menz, M. D., LaVail, M. M., and Flannery, J. G. (2000). Characterization of rhodopsin mis-sorting and constitutive activation in a transgenic rat model of retinitis pigmentosa. Invest. Ophthalmol. Vis. Sci. *41*, 1546–1553.

Hao, W., Wenzel, A., Obin, M. S., Chen, C. K., Brill, E., Krasnoperova, N. V., Eversole-Cire, P., Kleyner, Y., Taylor, A., Simon, M. I., Grimm, C., Reme, C. E., and Lem, J. (2002). Evidence for two apoptotic pathways in light-induced retinal degeneration. Nat. Genet. *32*, 254–260.

Hurd, D. D., and Saxton, W. M. (1996). Kinesin mutations cause motor neuron disease phenotypes by disrupting fast axonal transport in Drosophila. Genetics *144*, 1075–1085.

Illing, M. E., Rajan, R. S., Bence, N. F., and Kopito, R. R. (2002). A rhodopsin mutant linked to autosomal dominant retinitis pigmentosa is prone to aggregate and interacts with the ubiquitin proteasome system. J. Biol. Chem. *277*, 34150–34160.

Insinna, C., Humby, M., Sedmak, T., Wolfrum, U., and Besharse, J. C. (2009). Different roles for KIF17 and kinesin II in photoreceptor development and maintenance. Dev. Dyn. *238*, 2211–2222

Insinna, C., Pathak, N., Perkins, B., Drummond, I., and Besharse, J. C. (2008). The homodimeric kinesin, Kif17, is essential for vertebrate photoreceptor sensory outer segment development. Dev. Biol. *316*, 160–170

Jansen, H. G., Sanyal, S., De Grip, W. J., and Schalken, J. J. (1987). Development and degeneration of retina in rds mutant mice: ultraimmunohistochemical localization of opsin. Exp. Eye Res. *44*, 347–361.

Jimeno, D., Feiner, L., Lillo, C., Teofilo, K., Goldstein, L. S., Pierce, E., and Williams, D. S. (2006). Analysis of kinesin-2 function in photoreceptor cells using synchronous *Cre-loxP* knockout of *Kif3a* with RHO-Cre. Invest. Ophthalmol. Vis. Sci. *47*, 5039–5046.

Kamal, A., Stokin, G. B., Yang, Z., Xia, C. H., and Goldstein, L. S. (2000). Axonal transport of amyloid precursor protein is mediated by direct binding to the kinesin light chain subunit of kinesin-I. Neuron *28*, 449–459.

Kiselev, A., Socolich, M., Vinos, J., Hardy, R. W., Zuker, C. S., and Ranganathan, R. (2000). A molecular pathway for light-dependent photoreceptor apoptosis in Drosophila. Neuron *28*, 139–152.

Krock, B. L., and Perkins, B. D. (2008). The intraflagellar transport protein IFT57 is required for cilia maintenance and regulates IFT-particle-kinesin-II dissociation in vertebrate photoreceptors. J. Cell Sci. *121*, 1907–1915.

Lawrence, C. J., Dawe, R. K., Christie, K. R., Cleveland, D. W., Dawson, S. C., Endow, S. A., Goldstein, L. S., Goodson, H. V., Hirokawa, N., Howard, J., Malmberg, R. L., McIntosh, J. R., Miki, H., Mitchison, T. J., Okada, Y., Reddy, A. S., Saxton, W. M., Schliwa, M., Scholey, J. M., Vale, R. D., Walczak, C. E., and Wordeman, L. (2004). A standardized kinesin nomenclature. J. Cell Biol. *167*, 19–22.

Lem, J., Krasnoperova, N. V., Calvert, P. D., Kosaras, B., Cameron, D. A., Nicolo, M., Makino, C. L., and Sidman, R. L. (1999). Morphological, physiological, and biochemical changes in rhodopsin knockout mice. Proc. Natl. Acad. Sci. USA *96*, 736–741.

Li, T., Snyder, W. K., Olsson, J. E., and Dryja, T. P. (1996). Transgenic mice carrying the dominant rhodopsin mutation P347S: evidence for defective vectorial transport of rhodopsin to the outer segments. Proc. Natl. Acad. Sci. USA *93*, 14176–14181.

Lin-Jones, J., Parker, E., Wu, M., Knox, B. E., and Burnside, B. (2003). Disruption of kinesin II function using a dominant negative-acting transgene in *Xenopus laevis* rods results in photoreceptor degeneration. Invest. Ophthalmol. Vis. Sci. *44*, 3614–3621.

Lohr, H. R., Kuntchithapautham, K., Sharma, A. K., and Rohrer, B. (2006). Multiple, parallel cellular suicide mechanisms participate in photoreceptor cell death. Exp. Eye Res. *83*, 380–389.

Louie, C. M., Caridi, G., Lopes, V. S., Brancati, F., Kispert, A., Lancaster, M. A., Schlossman, A. M., Otto, E. A., Leitges, M., Grone, H. J., Lopez, I., Gudiseva, H. V., O'Toole, J. F., Vallespin, E., Ayyagari, R., Ayuso, C., Cremers, F. P., den Hollander, A. I., Koenekoop, R. K., Dallapiccola, B., Ghiggeri, G. M., Hildebrandt, F., Valente, E. M., Williams, D. S., and Gleeson, J. G. (2010). AHI1 is required for photoreceptor outer segment development and is a modifier for retinal degeneration in nephronophthisis. Nat. Genet. *42*, 175–180.

Lyubarsky, A. L., Daniele, L. L., and Pugh, E. N., Jr. (2004). From candelas to photoisomerizations in the mouse eye by rhodopsin bleaching in situ and the light-rearing dependence of the major components of the mouse ERG. Vision Res. *44*, 3235–3251.

Marszalek, J. R., Liu, X., Roberts, E. A., Chui, D., Marth, J. D., Williams, D. S., and Goldstein, L. S. (2000). Genetic evidence for selective transport of opsin and arrestin by kinesin-II in mammalian photoreceptors. Cell *102*, 175–187.

Nir, I., Agarwal, N., Sagie, G., and Papermaster, D. S. (1989). Opsin distribution and synthesis in degenerating photoreceptors of rd mutant mice. Exp. Eye Res. *49*, 403–421.

Nir, I., and Papermaster, D. S. (1986). Immunocytochemical localization of opsin in the inner segment and ciliary plasma membrane of photoreceptors in retinas of rds mutant mice. Invest Ophthalmol. Vis. Sci. *27*, 836–840.

Nir, I., Sagie, G., and Papermaster, D. S. (1987). Opsin accumulation in photoreceptor inner segment plasma membranes of dystrophic RCS rats. Invest. Ophthalmol. Vis. Sci. *28*, 62–69.

Nishimura, D. Y., Fath, M., Mullins, R. F., Searby, C., Andrews, M., Davis, R., Andorf, J. L., Mykytyn, K., Swiderski, R. E., Yang, B., Carmi, R., Stone, E. M., and Sheffield, V. C. (2004). Bbs2-null mice have neurosensory deficits, a defect in social dominance, and retinopathy associated with mislocalization of rhodopsin. Proc. Natl. Acad. Sci. USA *101*, 16588–16593.

Nusinowitz, S., Ridder, W. H., 3rd, and Ramirez, J. (2007). Temporal response properties of the primary and secondary rod-signaling pathways in normal and Gnat2 mutant mice. Exp. Eye Res. *84*, 1104–1114.

Papermaster, D. S., Converse, C. A., and Siuss, J. (1975). Membrane biosynthesis in the frog retina: opsin transport in the photoreceptor cell. Biochemistry *14*, 1343–1352.

Pazour, G. J., Baker, S. A., Deane, J. A., Cole, D. G., Dickert, B. L., Rosenbaum, J. L., Witman, G. B., and Besharse, J. C. (2002). The intraflagellar transport protein, IFT88, is essential for vertebrate photoreceptor assembly and maintenance. J. Cell Biol. *157*, 103–113.

Perlson, E., Maday, S., Fu, M. M., Moughamian, A. J., and Holzbaur, E. L. (2010). Retrograde axonal transport: pathways to cell death? Trends Neurosci. *33*, 335–344.

Rosenbaum, J. L., and Witman, G. B. (2002). Intraflagellar transport. Nat. Rev. Mol. Cell Biol. *3*, 813–825.

Scholey, J. M. (2008). Intraflagellar transport motors in cilia: moving along the cell's antenna. J. Cell Biol. *180*, 23–29.

Stokin, G. B., Lillo, C., Falzone, T. L., Brusch, R. G., Rockenstein, E., Mount, S. L., Raman, R., Davies, P., Masliah, E., Williams, D. S., and Goldstein, L. S. (2005). Axonopathy and transport deficits early in the pathogenesis of Alzheimer's disease. Science *307*, 1282–1288.

Strissel, K.J., Sokolov, M., and Arshavsky, V. (eds.) (2004). Light-Dependent Translocation of Signaling Proteins in Vertebrate and Invertebrate Photoreceptors. World Scientific Publishing: Singapore.

Strissel, K. J., Sokolov, M., Trieu, L. H., and Arshavsky, V. Y. (2006). Arrestin translocation is induced at a critical threshold of visual signaling and is superstoichiometric to bleached rhodopsin. J. Neurosci. *26*, 1146–1153.

Sukumaran, S., and Perkins, B. D. (2009). Early defects in photoreceptor outer segment morphogenesis in zebrafish ift57, ift88 and ift172 Intraflagellar Transport mutants. Vision Res. *49*, 479–489.

Sung, C. H., Davenport, C. M., Hennessey, J. C., Maumenee, I. H., Jacobson, S. G., Heckenlively, J. R., Nowakowski, R., Fishman, G., Gouras, P., and Nathans, J. (1991). Rhodopsin mutations in autosomal dominant retinitis pigmentosa. Proc. Natl. Acad. Sci. USA *88*, 6481–6485.

Sung, C. H., Makino, C., Baylor, D., and Nathans, J. (1994). A rhodopsin gene mutation responsible for autosomal dominant retinitis pigmentosa results in a protein that is defective in localization to the photoreceptor outer segment. J. Neurosci. *14*, 5818–5833.

Tam, B. M., and Moritz, O. L. (2006). Characterization of rhodopsin P23H-induced retinal degeneration in a *Xenopus laevis* model of retinitis pigmentosa. Invest. Ophthalmol. Vis. Sci *47*, 3234–3241.

Tam, B. M., Moritz, O. L., Hurd, L. B., and Papermaster, D. S. (2000). Identification of an outer segment targeting signal in the COOH terminus of rhodopsin using transgenic *Xenopus laevis*. J. Cell Biol. *151*, 1369–1380.

Tan, E., Wang, Q., Quiambao, A. B., Xu, X., Qtaishat, N. M., Peachey, N. S., Lem, J., Fliesler, S. J., Pepperberg, D. R., Naash, M. I., and Al-Ubaidi, M. R. (2001). The relationship between opsin overexpression and photoreceptor degeneration. Invest. Ophthalmol. Vis. Sci. *42*, 589–600.

Usukura, J., and Bok, D. (1987). Changes in the localization and content of opsin during retinal development in the rds mutant mouse: immunocytochemistry and immunoassay. Exp. Eye Res. *45*, 501–515.

Xu, J., Dodd, R. L., Makino, C. L., Simon, M. I., Baylor, D. A., and Chen, J. (1997). Prolonged photoresponses in transgenic mouse rods lacking arrestin. Nature *389*, 505–509.

Young, R. W. (1967). The renewal of photoreceptor cell outer segments. J. Cell Biol. *33*, 61–72.

Zhao, Y., Hong, D. H., Pawlyk, B., Yue, G., Adamian, M., Grynberg, M., Godzik, A., and Li, T. (2003). The retinitis pigmentosa GTPase regulator (RPGR)- interacting protein: subserving RPGR function and participating in disk morphogenesis. Proc. Natl. Acad. Sci.USA *100*, 3965–3970.